S. H. van Leeuwen, J. H. van Boon, *Tetrahedron Lett.* **1990**, *31*, 1331–1334.

[20] HPLC conditions: column: Millipore NovaPak C18, 4.6 × 150 mm; flow: 1.00 mL min^{-1}; detection: 254 nm; RT; solvents A: 10% CH_3CN in H_2O with 0.1% TFA, B: 10% H_2O in CH_3CN with 0.1% TFA, solvent gradient: 0 min (100% A), 5 min (50:50 A:B), 35 min (30:70 A:B), 45–55 min (100% B). Retention time: **2** (37.8 and 41.1 min), **3** (11.9 min), **5** (30.5 and 31.8 min), **6** (16.2 min), **8** (56.3 and 58.1 min), **9** (7.6 min).

[21] The yield was estimated from the peak area of the HPLC chromatogram and the molar absorbance of the benzyl and terephthalate groups.

Tuning the Semiconducting Properties of Sexithiophene by α,ω-Substitution—α,ω-Diperfluorohexylsexithiophene: The First n-Type Sexithiophene for Thin-Film Transistors[**]

Antonio Facchetti, Yvonne Deng, Anchuan Wang, Yoshihiro Koide, Henning Sirringhaus, Tobin J. Marks,[*] and Richard H. Friend[*]

$\alpha\alpha'$-Conjugated thiophene oligomers (nTs) and polymers (PTs) have attracted great interest as semiconducting elements in organic thin-film transistors (TFTs).[1, 2] To be useful in such structures, the organic material must support a channel of holes or electrons (p- or n-type semiconductor, respectively) created by the gate electrode bias, which switches the device "on". Furthermore, the charge mobility of the material must be sufficiently large to increase the source–drain on-conduction by many orders of magnitude over the "off" state. The most important examples of this family of compounds are unsubstituted, α,ω-, and β,β'-dialkylsubstituted nTs ($x = 1, 2$), and β-alkyl-substituted PTs, where optimized carrier mobilities (0.1–0.6 cm^2 V^{-1} s^{-1}) and on/off ratios ($>10^6$) approach those of amorphous silicon.[1e, 2a,c,e, 3] Without exception, these systems behave as p-type semiconductors, presumably because the electron-richness of the thiophene renders negative carriers susceptible to trapping by more electronegative residual impurities such as oxygen. On the other hand, developing and understanding new n-type materials would enable applications,[4] such as bipolar transistors, p-n junction diodes, and complementary circuits, as well as to afford a better fundamental understanding of charge transport in molecular solids. The major barrier to progress, however, is that most n-type organics are either environmentally sensitive, have relatively low field mobilities, lack volatility for efficient film growth, and/or are difficult to synthesize.[4, 5, 6]

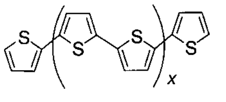
nT, 0 < x < 5

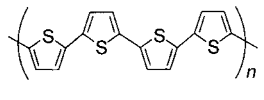
PT

We report here the facile, efficient synthesis of the first n-type sexithiophene conductor, α,ω-diperfluorohexylsexithiophene (DFH-6T; **1**), for TFTs. DFH-6T was synthesized by a Pd^0-catalyzed Stille coupling of 5-bromo-5'-perfluorohexyl-dithiophene (**6**) with 5,5'-di(tributylstannyl)dithiophene (Scheme 1). This route affords DFH-6T (**1**) in high purity and yield after multiple gradient sublimation. Although monosubstituted perfluoroalkyl thiophene oligomers with up to three units have been reported, synthetic yields were typically about 10%.[7]

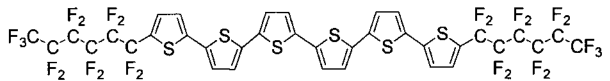
DFH-6T **1**

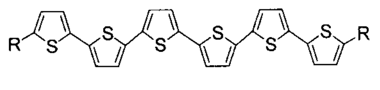
DH-6T **2**, R = n-C_6H_{13}
6T **3**, R = H

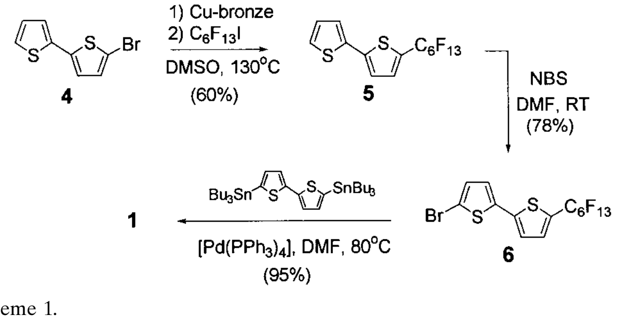

Scheme 1.

The comparative thermal properties of DFH-6T (**1**) and DH-6T (**2**) were investigated by differential scanning calorimetry (DSC) and thermal gravimetric analysis (TGA). The DSC trace of compound **1** exhibits a distinct crystal-to-liquid crystal (LC) transition at 292 °C and a LC-to-isotropic transition at 309 °C, while the crystal-to-LC transition of **2** (300 °C) falls just below the melting point, 308–313 °C.[8] These mesophase-formation events are not surprising in view

---

[*] Prof. T. J. Marks, Dr. A. Facchetti, Dr. A. Wang, Dr. Y. Koide
Department of Chemistry and the Materials Research Center
Northwestern University
2145 Sheridan Road, Evanston, IL, 60208-3113 (USA)
Fax: (+1) 847-491-2290
E-mail: tjmarks@casbah.acns.nwu.edu

Prof. R. H. Friend, Y. Deng, Dr. H. Sirringhaus
Cavendish Laboratory, Department of Physics
University of Cambridge
Madingley Road, Cambridge CB3 0HE (UK)
Fax: (+44) 1223-353297
E-mail: rhf10@cam.ac.uk

[**] We thank DARPA (N00421-98-1187) and the NSF-MRSEC program through the Northwestern Materials Research Center (DMR-9632472) for support of this research. H.S. thanks the Royal Society for a University Research Fellowship (URF).

of the molecular architectures. However, the most interesting feature is that the two systems exhibit such similar thermal behavior and almost identical melting points, which suggests that the strong π–π interactions of DH-6T[1a, 2b] are preserved upon substitution with fluoroalkyl groups. In contrast, the α,ω-fluorocarbon chains have a dramatic effect on the volatility of **1** (Figure 1A). The graph of the percentage weight retention versus the temperature for **2** demonstrates that a smooth, clean, quantitative sublimation occurs well below the melting point with negligible residue. In contrast, DH-6T (**1**) exhibits significant volatility only above the melting point. The TGA data reveal inflections at about 298 and 306 °C, which suggests decomposition processes occur. In addition, a significant decomposition-related residue (ca. 6%) is observed at 320 °C. The enhanced volatility and stability of DFH-6T relative to DH-6T is further demonstrated by isothermal TGA (Figure 1B), which shows that sublimation of DH-6T at the lowest possible temperature leaves about 8% of a decomposition residue.

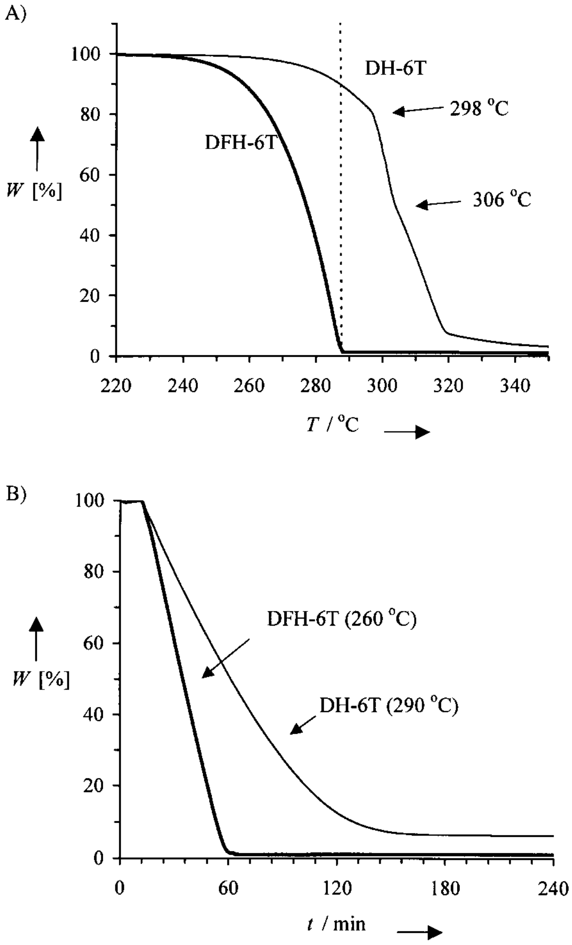

Figure 1. Comparison of the volatility characteristics of DHF-6T and DH-6T by TGA at reduced pressure (0.01 torr N_2). A) Comparison plots of the weight retention (w) for DH-6T and DFH-6T recorded at a ramp rate of 1.5 °C min^{-1}. B) Isothermal data collected at 260 and 290 °C for DFH-6T and DH-6T, respectively.

Figure 2 compares the optical absorption and emission (PL) spectra of DFH-6T and DH-6T in solution (Figure 2A) and as thin vapor-deposited films (Figure 2B). Remarkably, the solution spectra are nearly superimposable, which suggests that the energy differences between the ground and excited states of the 6T core are only marginally sensitive to α,ω-substitution and that the HOMO–LUMO gaps are nearly identical at approximately 2.4 eV. The spectra of the films exhibit both differences and similarities. First, both PL spectra have a central peak and two weaker shoulders. The high-energy shoulders fall, for both systems, at the same wavelength near the tail of the absorption, which yields estimated HOMO–LUMO gaps of about 2.2 eV in the films. However, while DFH-6T exhibits strong green fluorescence ($\lambda_{max} \approx$ 588 nm), the DH-6T emission intensity is several orders of magnitude weaker and red-shifted by about 30 nm. The low PL yields of thin films of DH-6T (**2**) and 6T (**3**) as well as the blue-shifted absorption maximum vs. that in solution were previously ascribed to Davydov splitting.[9–11] The origin of the blue-shifted absorption band in DFH-6T and enhanced PL efficiency is unknown and warrants further study. While both DH-6T and DFH-6T exhibit strong intermolecular π–π interactions, they are not isostructural (see below).

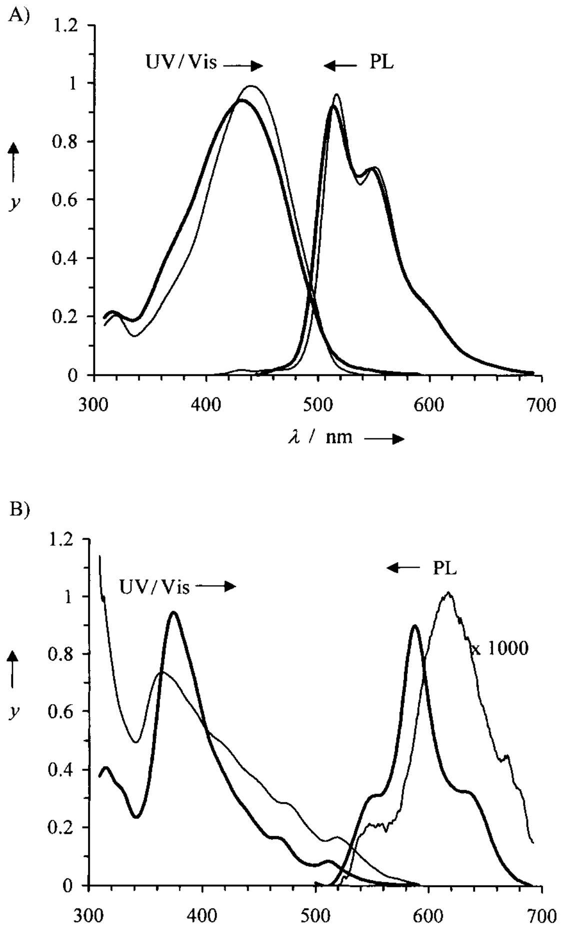

Figure 2. Optical absorption (UV/Vis) and emission (PL) spectra of DFH-6T (bold line) and DH-6T (fine line). A) As dilute solutions in toluene at approximately 80 °C. The PL spectra were obtained by exciting the solutions at 444 nm (DFH-6T) and 436 nm (DH-6T). B) As thin films (ca. 1.8 µm) on glass substrates. The PL spectra were recorded with excitation at 377 nm (DFH-6T) and 363 nm (DH-6T). Intensities (y) are in arbitrary units.

The electronic consequences of substituting of DH-6T with fluoroalkyl groups were also investigated by cyclic voltammetry (one-compartment cell with a Pt electrode, an Ag/0.1 M $AgNO_3$ (CH_3CN) reference, and an Ag counter electrode).[11] Voltammograms of DFH-6T (**1**) and DH-6T (**2**) in $CHCl_3$/0.10 M $TBABF_4$ (TBA = tetrabutylammonium) exhibit two chemically irreversible oxidative waves at $+0.68/+0.88$ V and $+0.41/+0.61$ V,[12] respectively, and negligible reductive features, which are indicative of chemically irreversible oxidative processes likely related to polaron and bipolaron formation.[13] The first and second anodic peaks of DFH-6T exhibit a uniform anodic shift (ca. $+0.27$ V) relative to those of DH-6T, which indicates that introduction of perfluoroalkyl chains on the 6T core substantially increases the ionization potential. The similar HOMO–LUMO gaps of **1** and **2** (see above) indicate that the LUMO of **1** is also approximately 0.27 V below that of **2**, which is confirmed by electrochemical studies on thin films.[14] Low solubility limits reductive studies by conventional cyclic voltammetry. Recently, Katz et al. reported that substitution with fluorinated R^FCH_2 groups improves the air stability and solubility of a well-known n-type naphthalenetetracarboxylic acid diimide while affording mobilities of up to 0.1 $cm^2V^{-1}s^{-1}$.[15] The perfluoroalkyl chain is not in direct communication with the π system, and electronic effects should be substantially attenuated.

Scanning electron microscopy (SEM) studies reveal that the growth of the DFH-6T film depends significantly on the substrate temperature and surface pretreatment. Films deposited at 25 °C consist of small crystalline grains (ca. 80×50 nm^2) resulting from rapid condensation on the cold substrate (Figure 3 A), while growth at 85 °C affords elongated grains with larger dimensions (ca. 500×60 nm^2) and random orientation. Growth at 145 °C yields larger crystallites (Figure 3 B; ca. 1000×350 nm^2), however, film morphology is less smooth, probably because the volatility of DFH-6T prevents its uniform adsorption on the hot surface. The influence of the substrate temperature on crystallite size and film morphology for other thiophene semiconductors such as 6T (**3**)[13] is known to be related to nucleation site density, growth rate, and surface free energy phenomena during growth.[16] Since Si/SiO_2 has a hydrophilic native oxide layer, the surface is not ideal for the deposition of a hydrophobic adsorbate. Thus, substrates were also pretreated with $CF_3(CF_2)_5CH_2CH_2SiCl_3$ to produce a fluorocarbon monolayer. The crystallite dimensions are increased by approximately 10 % and the grain-to-grain and grain-to-substrate interconnections are visibly enhanced.

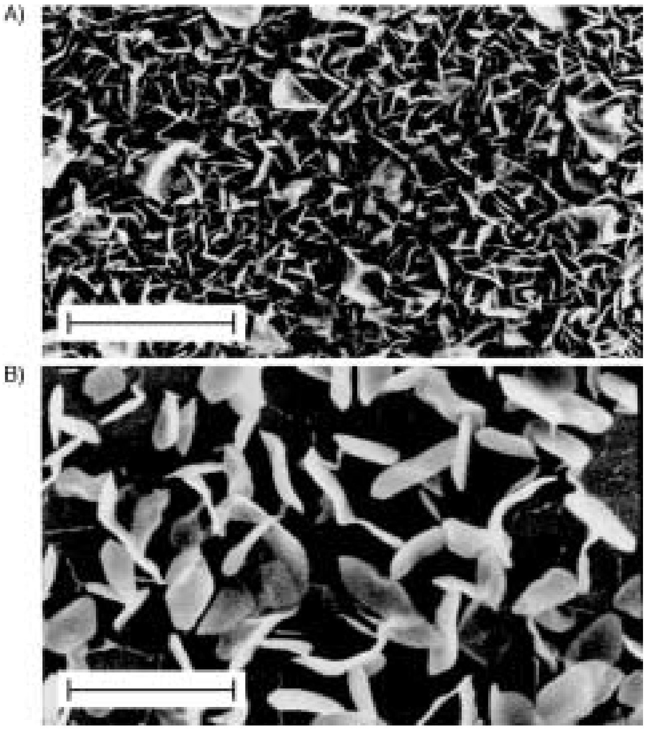

Figure 3. SEM images (2 kV × 15.0 K) of 100-nm thick DFH-6T films deposited on silicon at substrate temperatures of: A) 25 °C, B) 145 °C. Bars represent 2 μm.

X-ray diffraction ($Cu_{K\alpha}$) scans of DFH-6T films grown at various temperatures (Figure 4) reveal that higher crystalline order is achieved as the substrate temperature is increased to 200 °C. Annealing the films at 240 °C further enhances microstructural alignment, with the dominant Bragg features assignable to a family of (*n*00) reflections corresponding to a real-space periodicity of 36.1 ± 0.2 Å. This value is close to the reported DFH-6T monolayer thickness (35.5 Å). Although the crystal structure of DFH-6T has not been determined, the XRD data suggest a preferential molecular orientation with the long axes along the substrate normal, where transport in the plane of the film would benefit from close π–π stacking. The DFH-6T films grown on Si substrates treated with $CF_3(CF_2)_5CH_2CH_2SiCl_3$ exhibit sharper XRD reflections, which is indicative of more highly ordered films. Finally, powder diffraction reveals that DFH-6T and DH-6T are not isostructural; different unit cell arrangements are expected in view of the different packing characteristics of hydrocarbon versus perfluorocarbon chains.[17]

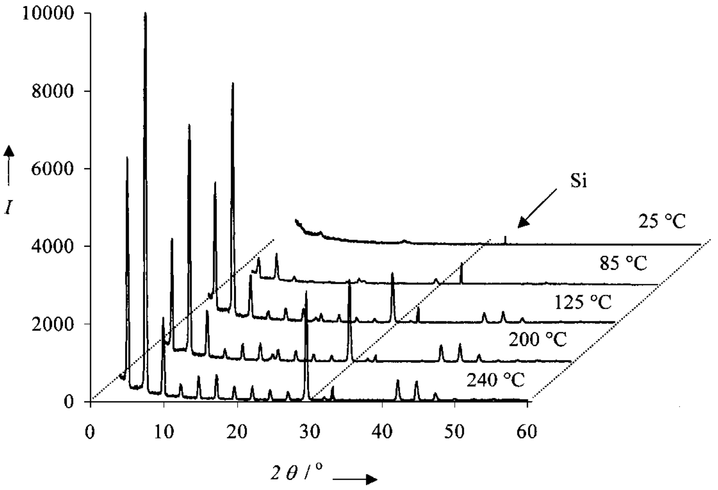

Figure 4. X-ray $\theta-2\theta$ diffractograms of approximately 2 μm-thick vacuum-evaporated DFH-6T films grown on Si substrates at various substrate temperatures. The spectrum recorded at 240 °C corresponds to a film grown at 200 °C and annealed at 240 °C for 30 min.

Field-effect measurements were carried out on top-contact TFTs consisting of 30–100 nm films of DFH-6T deposited at less than 10^{-6} mbar and at approximately 0.5–1.0 Ås^{-1} onto

n^+-Si field-effect transistor (FET) substrates with a 230 nm dry thermal SiO_2 insulating layer. The substrate temperature was varied between 50 and 120 °C. The SiO_2 surface was silylated with hexamethyldisilazane[18] or $CF_3(CF_2)_5$-$CH_2CH_2SiCl_3$ prior to DFH-6T deposition; both yielded similar TFT results. The devices were completed by evaporating Au or Al source–drain contacts onto the DFH-6T layer. The device characteristics were measured under N_2 with an HP parameter analyzer. Figure 5 A shows the characteristics of a typical DFH-6T FET with Au source–drain contacts. Transistor action is observed only for positive gate voltages ($V_g > 0$), which indicates that a layer of mobile electrons accumulates at the interface between DFH-6T and SiO_2. No transistor action is induced by applying a negative gate voltage. Only p-type accumulation ($V_g < 0$) has previously been observed in TFTs of alkyl-substituted and unsubstituted oligo- and polythiophene derivatives. The present contrasting n-type conduction doubtless reflects the greater electron affinity of the fluoroalkyl-substituted sexithiophene. It is remarkable that this relatively minor change in the substituent is sufficient to dramatically alter the thin-film semiconducting properties from p- to n-type. To our knowledge, the only other example of such a sign inversion in the majority carrier is the phthalocyanine → perfluorophthalocyanine (F16Pc) system.[19] However, DFH-6T and M(F16Pc) differ markedly in the nature of their substituent effects. In the latter, extensive C–H → C–F substitution leads to large electronic perturbations of the core structure. Furthermore, the nature of the substituents differs. Whereas perfluoroalkyl chains exhibit only strong σ-inductive electron-withdrawing effects (−I), F atoms attached directly to π systems exhibit both donating-resonance (+M) and attracting-inductive (−I) characteristics.[20]

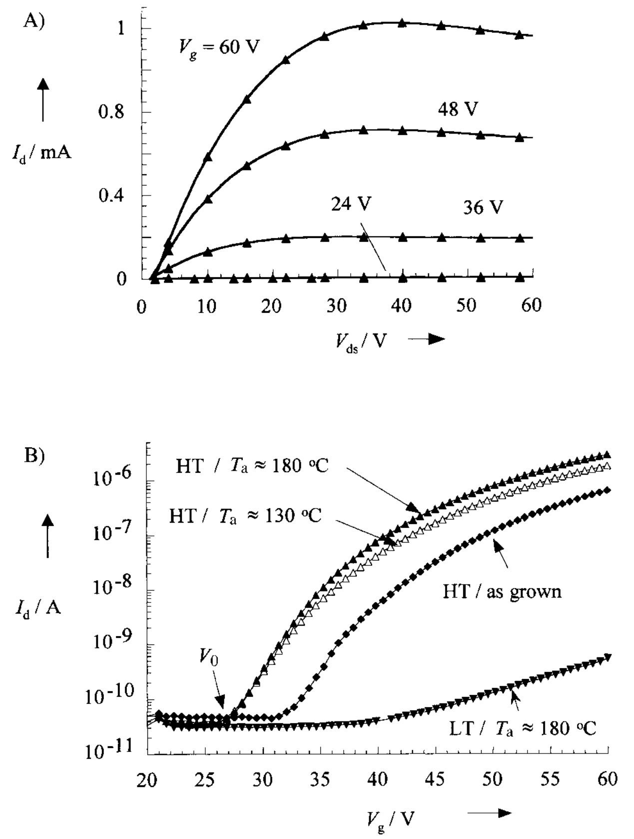

Figure 5. A) Output characteristics of a DFH-6T TFT with Au source–drain contacts deposited at a temperature of about 90 °C (channel length $L = 75\ \mu m$, $W = 1.5$ mm). B) Transfer characteristics of devices grown at a low temperature of 50 °C (LT: ▽), and a high temperature of approximately 90 °C (HT). The device characteristics shown at high temperature were measured directly after film growth (as-grown, ◆), and after post-growth annealing in vacuum at 130 °C (△), and 180 °C (▲).

The device of Figure 5 was fabricated with Au source–drain contacts. Devices with Al contacts exhibit similar characteristics, which is surprising considering the significantly higher work function of Au(5.1 eV) compared to that of Al (4.3 eV), which implies, a priori, there is a higher barrier for electron injection from Au. Similar injection effects have recently been reported for other n-type systems, and are not understood at present.[21] Values for the field-effect mobility were determined from the transfer characteristics in the saturation regime (Figure 5 B).[22] The highest mobilities of 0.02 $cm^2 V^{-1} s^{-1}$ were obtained for film growth at 80–100 °C [Equation (1)].

$$\frac{dI_d}{dV_g} = \frac{C_i W}{L} \mu_{FET}^{sat}(V_g)(V_g - V_T) \qquad (1)$$

Significantly lower mobilities ($< 10^{-4}\ cm^2 V^{-1} s^{-1}$) are observed for growth temperatures of approximately 50 °C, and a reduced mobility is also obtained for growth temperatures of 120 °C. This optimum substrate temperature doubtless reflects, among other factors, the dependence of the grain size distribution in the polycrystalline film on the temperature.[23] The on:off ratio in these DFH-6T devices is as high as 10^5:1. The devices exhibit relatively high turn-on voltages V_o of 25–35 V, which indicates a certain fraction of the induced electron carriers occupies localized trap states. The turn-on voltage increases further during operation. This increase results in a decrease of the TFT on-current as a function of time which manifests itself in a nonideal negative slope of the output characteristics in the saturation regime (Figure 5 A). The turn-on voltage can be somewhat reduced and stabilized by post-growth annealing (Figure 5 B).

These results demonstrate that functionalization of the 6T core with fluoroalkyl groups to give DFH-6T (**1**) substantially enhances thermal stability, volatility, and electron affinity relative to DH-6T (**2**) and affords the first n-type oligothiophene TFT. The morphology of the DFH-6T film is sensitive to substrate temperature and surface pretreatment, with crystallite size increasing with increasing growth temperature. UV/Vis, PL, and XRD studies indicate that while DFH-6T has close intermolecular π-stacking interactions, it is not isostructural with DH-6T. Since thiophene oligomers are typically p-type, the present work may provide a pathway by which all-oligothiophene complementary circuits can be realized.

Experimental Section

The reagents 5-bromo-2,2′-dithiophene (**4**),[24] and 5,5′-bis(tri-*n*-butylstannyl)-2,2′-dithiophene[25] were prepared according to known procedures. Solvents and chemicals were purchased from Aldrich or Lancaster and purified as required.

5: A suspension of Cu bronze (3.38 g, 53.16 mmol) in dry DMSO (30 mL) was heated at 125 °C for 15 min under nitrogen. Perfluorohexyl iodide (11.34 g, 25.43 mmol) was added dropwise in such a way as to keep the temperature below 135 °C. After 45 min, a solution of 5-bromodithiophene (2.50 g, 10.17 mmol) in the same solvent (7.0 mL) was added dropwise, and the reaction mixture was stirred at 125 °C for 16 h. The reaction was next quenched with cold water (100 mL) and diethyl ether was added (200 mL). After shaking the mixture, it was filtered through celite and the organic phase collected. The aqueous layer was extracted once more with diethyl ether (100 mL) and the two organic phases were combined, washed with water, and dried over $MgSO_4$. After filtration, the solvent was evaporated to yield a solid (5.18 g), which was chromatographed on silica gel (hexane) to afford pure product as a yellow solid (2.90 g, 5.99 mmol, 58.9 % yield). m.p. 51–53 °C (MeOH); ^1H NMR ($CDCl_3$): $\delta = 7.31-7.37$ (m, 2H), 7.28 (d, $^2J(H,H) = 3.6$ Hz, 1H), 7.18 (d, $^2J(H,H) = 3.7$ Hz, 1H), 7.06 (dd, $^2J(H,H) = 4.1$ Hz, 1H); ^{19}F NMR ($CDCl_3$): $\delta = -81.07$ (3F), -101.64 (2F), -121.83 (br, 4F), -123.11 (2F), -126.43 (2F). Elemental analysis calcd for $C_{14}H_5F_{13}S_2$ (%): C 34.72, H 1.04, F 51.00; found: C 34.96, H 0.99, F 49.95; HR-MS (EI, 70 eV) for $C_{14}H_5F_{13}S_2$ [M^+]: calcd: 483.9625, found: 483.9626.

6: With exclusion of light, *N*-bromosuccinimide (1.02 g, 5.73 mmol) was added to a solution of 5-perfluorohexyldihiophene (2.32 g, 4.79 mmol) in DMF (32 mL). After stirring the reaction mixture overnight at 25 °C, it was poured into brine (120 mL), and the solution then extracted with diethyl ether (3 × 100 mL). The organic phase was next washed with water, dried over $MgSO_4$, filtered, and the solvent evaporated to afford 2.60 g of crude product. Flash chromatography on silica gel (hexane) afforded **6** as a light yellow solid (2.10 g, 3.73 mmol, 77.8 % yield). Sublimation (50 °C/10^{-3} Torr) afforded a purer sample. m.p. 63–65 °C; ^1H NMR ($CDCl_3$) $\delta = 7.34$ (d, $^2J(H,H) = 3.1$ Hz, 1H), 7.12 (d, $^2J(H,H) = 3.1$ Hz, 1H), 7.03 (d, $^2J(H,H) = 3.3$ Hz, 1H), 7.01 (d, $^2J(H,H) = 3.3$ Hz, 1H); ^{19}F NMR ($CDCl_3$) $\delta = -81.21$ (3F), -101.87 (2F), -122.02 (br, 4F), -123.27 (2F), -126.56 (2F). Elemental analysis calcd for $C_{14}H_4BrF_{13}S_2$ (%): C 29.86, H 0.72, F 43.86; found: C 29.83, H 0.69, F 44.01; HR-MS (EI, 70 eV) for $C_{14}H_4BrF_{13}S_2$ [M^+]: calcd: 563.8709, found: 563.8721.

1: A mixture of 5,5′-bis(tri-*n*-butylstannyl)-2,2′-dithiophene (1.40 g, 1.88 mmol), 5-perfluorohexyl-5′-bromo-2,2′-dithiophene (2.00 g, 3.55 mmol), and [$Pd(PPh_3)_4$] (0.050 g, 0.040 mmol) in dry DMF (40 mL) was deareated twice with nitrogen. The reaction mixture was then heated at 80 °C for 7 h during which time a precipitate formed. After cooling, the bright orange solid was collected and washed several times with hexane, methanol, and acetone to afford the product (1.91 g, 1.69 mmol, 95.2 % yield), m.p. 309 °C. Additional purification can be achieved by multiple gradient sublimation. Elemental analysis calcd for $C_{36}H_{12}F_{26}S_6$ (%): C 38.24, H 1.07, F 43.69; found: C 38.16, H 1.15, F 43.42; MS (EI, 70 eV): m/z: 1127.4 ([M^+], 70 %).

Received: May 23, 2000
Revised: September 20, 2000 [Z15158]

---

[1] a) G. Horowitz, F. Kouki, A. El Kassmi, P. Valat, V. Wintgens, F. Garnier, *Adv. Mater.* **1999**, *11*, 234; b) F. Garnier, R. Hajaoui, A. El Kassmi, G. Horowitz, L. Laigre, W. Porzio, M. Armanini, F. Provasoli, *Chem. Mater.* **1998**, *10*, 3334; c) X. C. Li, H. Sirringhaus, F. Garnier, A. B. Holmes, S. C. Moratti, N. Feeder, W. Clegg, S. J. Teat, R. H. Friend, *J. Am. Chem. Soc.* **1998**, *120*, 2206; d) G. Horowitz, F. Kouki, F. Garnier, *Adv. Mater.* **1998**, *10*, 382; e) G. Horowitz, *Adv. Mater.* **1998**, *10*, 365.

[2] a) W. Li, H. E. Katz, A. J. Lovinger, J. G. Laquindanum, *Chem. Mater.* **1999**, *11*, 458; b) H. E. Katz, J. G. Laquindanum, A. J. Lovinger, *Chem. Mater.* **1998**, *10*, 633; c) J. G. Laquindanum, H. E. Katz, A. J. Lovinger, *J. Am. Chem. Soc.* **1998**, *120*, 664; d) T. Siegrist, C. Kloc, R. A. Laudise, H. E. Katz, R. C. Haddon, *Adv. Mater.* **1998**, *10*, 379; e) H. E. Katz, *J. Mater. Chem.* **1997**, *7*, 369.

[3] a) H. Sirringhaus, P. J. Brown, R. H. Friend, K. Bechgaard, B. M. W. Lengeveld-Voss, A. J. H. Spiering, R. A. J. Janssen, E. W. Meijer, P. Herving, D. M. de Leeuw, *Nature* **1999**, *401*, 685; b) G. Barbarella, M. Zambianchi, L. Antolini, P. Ostoja, P. Maccagnani, A. Bongini, E. A. Marseglia, E. Tedesco, G. Gigli, R. Cingolani, *J. Am. Chem. Soc.* **1999**, *121*, 8920; c) J. H. Shön, C. Kloc, R. A. Laudise, B. Batlogg, *Appl. Phys. Lett.* **1998**, *73*, 3574.

[4] a) Y.-Y. Lin, A. Dodabalapur, R. Sarpeshkar, Z. Bao, W. Li, K. Baldwin, V. R. Raju, H. E. Katz, *Appl. Phys. Lett.* **1999**, *74*, 2714; b) G. Horowitz, *Adv. Mater.* **1998**, *10*, 365; c) A. Dodalabapur, J. G. Laquindanum, H. E. Katz, Z. Bao, *Appl. Phys. Lett* **1996**, *69*, 4227; d) N. C. Greenham, S. C. Moratti, D. D. C. Bradley, R. H. Friend, *Nature* **1993**, *365*, 628.

[5] a) C. P. Jarret, K. Pichler, R. Newbould, R. H. Friend, *Synth. Met.* **1996**, *77*, 35; b) R. C. Haddon, *J. Am. Chem. Soc.* **1996**, *118*, 3041; c) G. Horowitz, F. Kouki, P. Spearman, D. Fichou, C. Nogues, X. Pan, F. Garnier, *Adv. Mater.* **1996**, *8*, 242; d) J. G. Laquindanum, H. E. Katz, A. Dodalabapur, A. J. Lovinger, *J. Am. Chem. Soc.* **1996**, *118*, 11 331.

[6] The transport properties of metal/α,ω-dicyano-6HT/metal structures are highly metal/interface dependent; TFT carrier signs and mobilities have not been reported: F. Demanze, A. Yassar, D. Fichou, *Synth. Met.* **1999**, *101* 620.

[7] L. Robitaille, M. Leclerc, *Macromolecules* **1994**, *27*, 1847.

[8] H. E. Katz, A. Dodalabapur, L. Torsi, D. Elder, *Chem. Mater.* **1995**, *7*, 2238.

[9] a) F. Garnier, *Acc. Chem. Res.* **1999**, *32*, 209; b) A. Yassar, G. Horowitz, P. Valat, V. Wintgens, M. Hmyene, F. Deloffre, P. Srivastava, P. Lang, F. Garnier, *J. Phys. Chem.* **1995**, *99*, 9155; c) A. Yassar, P. Valat, V. Wintgens, M. A. Hmyene, F. Deloffre, G. Horowitz, P. Srivastava, F. Garnier, *Synth. Met.* **1994**, *67*, 277.

[10] M. Pope, C. E. Swenberg, *Electronic Processes in Organic Crystals*, Oxford University Press, New York, **1982**.

[11] The Ag/$AgNO_3$ reference electrode was additionally calibrated against ferrocene/ferrocinium ($E_{1/2} = 0.042$ V).

[12] Electrochemical studies on DH-6T: B. Nessakh, G. Horowitz, F. Garnier, F. Deloffre, P. Srivastava, A. Yassar, *J. Electroanal. Chem.* **1995**, *399*, 97. Our oxidative results in $CHCl_3$ are in agreement.

[13] a) R. Cervini, X. C. Li, G. W. C. Spencer, A. B. Holmes, S. C. Moratti, R. H. Friend, *Synth. Met.* **1997**, *84*, 359; b) M. Helbig, H.-H. Horhold, *Makromol. Chem.* **1993**, *194*, 1607.

[14] A. Facchetti, Y. Koide, T. J. Marks, unpublished results.

[15] H. E. Katz, A. J. Lovinger, J. Johnson, C. Kloc, T. Siegrist, W. Li, Y.-Y. Lin, A. Dodabalapur, *Nature* **2000**, *404*, 478.

[16] a) A. J. Lovinger, D. D. Davis, A. Dodabalapur, H. E. Katz, L. Torsi, *Macromolecules* **1996**, *29*, 4952; b) B. Servet, G. Horowitz, S. Ries, O. Lagorsse, P. Alnot, A. Yassar, F. Deloffre, P. Srivastava, R. Hajaoui, P. Lang, F. Garnier, *Chem. Mater.* **1994**, *6*, 1809.

[17] H. Tadokoro, *Structure of Crystalline Polymers*, Wiley, New York, **1979**.

[18] H. Sirringhaus, N. Tessler, R. H. Friend, *Synth. Met.* **1999**, *102*, 857.

[19] Z. Bao, A. J. Lovinger, J. Brown, *J. Am. Chem. Soc.* **1998**, *120*, 207.

[20] *The Chemistry of the Carbon–Hydrogen Bond* (Ed.: S. Patai), Wiley, London, **1973**.

[21] a) J. H. Schön, S. Berg, C. Kloc, B. Battlogg, *Science* **2000**, *287*, 1022; b) B. Crone, A. Dodabalapur, Y.-Y. Lin, R. W. Filas, Z. Bao, A. LaDuca, R. Sarpeshkar, H. E. Katz, *Nature* **2000**, *403*, 521.

[22] H. Sirringhaus, N. Tessler, D. S. Thomas, P. J. Brown, R. H. Friend, *Adv. Solid State Physics* **1999**, *39*, 101.

[23] J. G. Laquindanum, H. E. Katz, A. J. Lovinger, *J. Am. Chem. Soc.* **1998**, *120*, 664.

[24] P. Bäuerle, F. Würthner, G. Götz, F. Effenberger, *Synthesis* **1993**, *11*, 1099.

[25] Y. Wei, Y. Yang, J.-M. Yeh, *Chem. Mater.* **1996**, *8*, 2659.